Modifications, Surface Morphology, and Mineral Composition of Clay Obtained from Southern Nigeria

Ukeme O. Isaac, **Ibanga O. Isaac**[*], **Itoro E. Willie**, **Etiyene I. Essiet**, **Rasheed Babalola, and Udo J. Ibok**

Abstract: The concept of green chemistry has in recent times played a vital role in the processing of feedstocks from locally sourced materials for the production of vast industrial products. This has, to a greater extent, resulted in the sustainability of a greener environment and economy. This research aimed to evaluate the mineral composition, characterization, and modifications of clay obtained from southern Nigeria. The clay sample collected at Ikot Ekang, Etinan Local Government Area, Akwa Ibom State, Nigeria, was leached with a mixture of concentrated tetraoxosulphate (VI) acid and trioxonitrate (V) acid (4:1 v/v) to obtain acid-leached clay (AC). The acid-treated clay was calcined at a high temperature of 1050 °C for 2 hours to obtain modified calcined clay (CC). The untreated clay was labeled OC. The surface characteristics, functional groups, minerals, oxides, and elemental compositions of OC, AC, and CC were evaluated using standard methods. The OC and AC show three absorption bands at 3623–3693.8 cm^{-1} regions. These peaks were absent in the CC sample. There was no significant difference at $p < 0.05$ in the mineral composition among the OC, AC, and CC samples, and the p-value was 0.999958. The Pearson correlation coefficient shows that the minerals of sample CC were strongly positively correlated with those of OC ($R = 0.774$; $R^2 = 0.5991$) and AC ($R = 0.9436$; $R^2 = 0.8904$). The percentage of quartz, syn, muscovite, and orthoclase minerals in OC, AC, and CC varied between 31–56%, 8.1–23%, and 1.87–9.8%, respectively. The surface morphology of the OC sample was plate-like, while surface porosity increased from AC to CC. The clay sample from southern Nigeria is mainly kaolinite clay, and the modification of clay through leaching with acid and calcination improves the mineral composition and quality of the clay minerals.

Ukeme O. Isaac
Department of Chemical/Petrochemical Engineering, Akwa Ibom State University, P.M.B. 1167, Uyo, Akwa Ibom State, Nigeria.
E-mail: ukemeisaac2018@gmail.com

[a,b]**Ibanga O. Isaac**[*]
[a]*Department of Chemistry, Akwa Ibom State University, P.M.B. 1167, Uyo, Akwa Ibom State, Nigeria*
[b]*Department of Chemical Sciences, Ritman University, P.O. Box 1321, Ikot Ekpene, Akwa Ibom State, Nigeria.*
Email: ibangaisaac@aksu.edu.ng
Orcid id: 0000-0003-0672-8783

Itoro E. Willie
[b]*Department of Chemistry, Akwa Ibom State University, P.M.B. 1167, Uyo, Akwa Ibom State, Nigeria*
Email: itoro_willienyakno@yahoo.com

Etiyene I. Essiet
Department of Chemistry, Akwa Ibom State University, P.M.B. 1167, Uyo, Akwa Ibom State, Nigeria
E-mail: eetiyene@gmail.com

Rasheed Babalola
Department of Chemical/Petrochemical Engineering, Akwa Ibom State University, P.M.B. 1167, Uyo, Akwa Ibom State, Nigeria.
E-mail: rasheedbabalola@aksu.edu.ng

Udo J. Ibok
Department of Chemistry, Akwa Ibom State University, P.M.B. 1167, Uyo, Akwa Ibom State, Nigeria
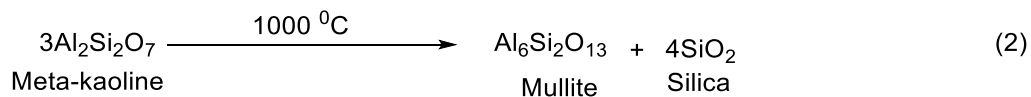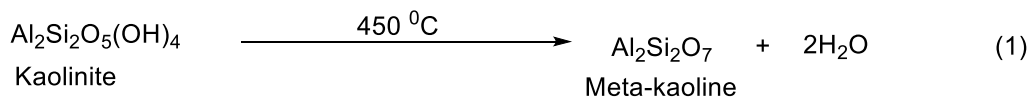**E-mail**: ibokuj@yahoo.com

1.0   Introduction

One of the essential components of ceramics is clay. It is a weathering product of natural sedimentary rocks and other types of primary rocks and is a common soil component, consisting mainly of crystalline particles of one or more minerals that are structurally different from one another and are known as clay minerals (CMs) (Wu *et al*., 2023; Ruiz *et al*., 2023; Ekpa and Isaac, 2008; Stocchi, 1990). Clay can be classified based on the ratios of CMs as montmorillonite when the ratio of montmorillonite and kaolinite minerals is 2:1, while kaolin clay is classified when the ratio of the above-mentioned CMs is 1:1 (Wu *et al*., 2023). Nascimento *et al*. (2016) also referred to clay as a natural, fine-grained mineral with plastic behaviour at appropriate water contents that will harden when fired or dried and is primarily hydrated aluminosilicates in which magnesium and iron can replace the aluminum wholly or partly with alkaline or alkaline earth elements.

Also present in the clay are rare earth elements (REE), among which are lanthanum (La), cerium (Ce), praseodymium (Pr), neodymium (Nd), promethium (Pm), samarium (Sm), europium (Eu), gadolinium (Gd), terbium (Tb), dysprosium (Dy), holmium (Ho), erbium (Er), thulium (Tm), ytterbium (Yb), lutetium (Lu), scandium (Sc), and yttrium (Y) that are often referred to as "industrial vitamins" (Xu *et al*., 2021). REE are essential components of functional materials such as fluorescence, magnetism, and hydrogen storage materials for use in various fields, such as aerospace, mobile communication, new energy, energy conservation, and industry (Wu *et al*., 2023). The stronger hydrophilicity property of CMs (Shi *et al*., 2023) could enhance their application as reinforcing agents in the preparation of water-dispersible alkyd resin biopolymer composites for use as binders in emulsion coatings. Clay and clay minerals in polymers or other materials can also improve the mechanical, thermal, barrier, and fire retardancy properties of the polymer (Gogoi *et al*., 2014). The use of acid-activated clay as an alternative material for bleaching palm oil has been reported (Ekpa and Isaac, 2008; Isaac *et al*., 2020).

The two main groups of clay minerals are the kaolins and the montmorillonites. The kaolins have the empirical formula $Al_2Si_2O_5(OH)_4$, while that of montmorillonites is $Al_2Si_4O_{10}(OH)_2$. The kaolin group includes kaolinite, nacrite, dickite, and halloysite; halloysite can also exist in a hydrated form having the formula $Al_2Si_2O_5(OH)_4.2H_2O$ (Worral, 1982). When kaolinite, nacrite, or dickite CMs are heated above 450 °C, meta-kaolin is formed (Equation 1) that behaves as if it were simply a mixture of finely divided silica and alumina. When CMs are heated over about 1000 °C, the products are mullite and free silica, which may be represented as shown in Equation 2 (Worrall, 1982).

$$Al_2Si_2O_5(OH)_4 \xrightarrow{\;450\,^{0}C\;} Al_2Si_2O_7 \;+\; 2H_2O \qquad (1)$$

Kaolinite   Meta-kaoline

$$3Al_2Si_2O_7 \xrightarrow{\;1000\,^{0}C\;} Al_6Si_2O_{13} + 4SiO_2 \qquad (2)$$

Meta-kaoline   Mullite   Silica

Clay minerals are critical components for fired bricks because they provide plasticity, porosity, and adequate strength for the desired products (Wang *et al*., 2022). Lei *et al*. (2022) characterize the clay minerals in the Sichuan Basin to consist mainly of detrital smectite, I/S and illite, authigenic talc, and Mg-smectite that transformed from sepiolite, in which Mg originated from high-Mg^{2+} parent calcites and Si was due to seawater mixing with $<\sim$5% terrigenous and $<\sim$0.05% hydrothermal contributions. Also, literature shows that the Middle Permian limestone marl alternations (LMAs) in South China are not only rich in smectites, illites, and I/S but also contain large amounts of authigenic Mg-phyllosilicates, such as sepiolites, talcs,

kerolites, Mg-smectites (stevensites), and mixed layers (Lei *et al.*, 2022; Gao *et al.*, 2020; Su *et al.*, 2020; Cai *et al.*, 2019: Li *et al.*, 2018).

The effects of natural and calcined halloysite clay minerals as low-cost additives on the performance of 3D-printed alkali-activated materials have been reported (Chougan *et al.*, 2022). The results show that the calcined halloysite clay at 1.5 wt% enhances the performance of the 3D printing in terms of shape stability, buildability, and mechanical properties as compared to the control mixture. Also, incorporating 0.5 wt% of attapulgite nano-clay in the alkali-activated materials increased thixotropic behaviour and 3D printing performance (Panda *et al.*, 2019).

Gelatin is a biodegradable, biocompatible, and low-production-cost protein material, but this biopolymer on its own has poor mechanical properties that limit its application in bioengineering systems. But with the emergence of nanoclay composites, there has been a tremendous improvement in the properties of this biopolymer in terms of mechanical and thermal properties (Pour-Esmaeil *et al.*, 2014).

Nigeria, mostly the southern part, is endowed with natural resources ranging from agricultural resources, medicinal plants (Isaac *et al.*, 2022a; Isaac *et al.*, 2022b), and mineral resources that are untapped due to the dependence of her economy on crude oil alone. It is therefore important for scientific, economic, and development sustainability to explore and exploit this important raw material, clay, in the southern part of Nigeria. Hence, this study is aimed at characterizing and processing clay via acid leaching and calcination obtained from the southern part of Nigeria.

2.0 Materials and methods
2.1 Sample collection and pre-treatment

The basin in which the clay minerals were collected was located at a road construction site along Ikot Ekang, Etinan Local Government Area of Akwa Ibom State, Nigeria (Figs. 1a and 1b). The clay sample was collected in a polyethylene bag and taken to the department of chemistry laboratory at Akwa Ibom State University. Pre-treatment of the clay sample was carried out based on the method described in the literature (Ewis *et al.*, 2022) with slight modifications. 500 g of the clay minerals were macerated in 2000 ml of distilled water and stirred with a mechanical stirrer for 1 hour to obtain a uniform mixture. The mixture was filtered with muslin cloth folded many times to obtain the finest clay particle size. The filtrate was dried in an oven and pulverized to obtain a powdered clay sample that was referred to as ordinary clay (OC).
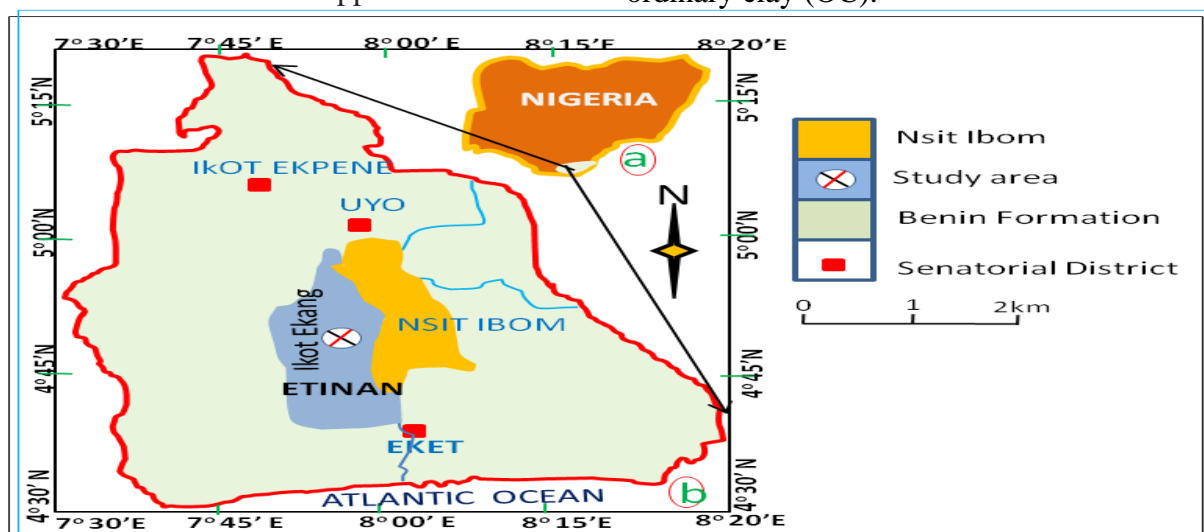

Fig. 1a Map of the study area

Fig. 1b Road construction site along Ikot Ekang, Etinan L.G.A., Akwa Ibom State-Nigeria

2.2 Acid leaching of the clay mineral

The clay sample was leached with aqua regia prepared following a literature report (Gogoi *et al*., 2014) with slight modifications as follows: A 500-ml mixture of concentrated tetraoxosulphate (VI) acid and trioxonitrate (V) acid (4:1, v/v) was prepared by slowly adding 100 ml of trioxonitrate (V) acid to 400 ml of concentrated tetraoxosulphate (VI) acid. The clay sample, 50 g, was treated with 160 ml of freshly prepared aqua regia at ambient temperature. The mixture was stirred continuously for 16 hours. The acid-treated clay was washed with distilled water until neutral. It was then dried in an oven at 105 °C to remove any remaining water. The dried sample was labeled "AC".

2.3 Calcination of acid-leached clay

The acid-leached clay sample was calcined in a laboratory furnace at a temperature of 1050 °C for 2 hours (Worrall, 1982) to eliminate water molecules and obtain a fine sample of clay mineral that was labelled CC. This was preserved in a plastic bottle for analysis.

2.4 Instruments and measurements
2.4.1 Fourier Transform Infrared Spectroscopy (FT-IR)

The FT-IR of samples OC, AC, and CC was recorded in the FTIR Nicolet, Impact 410 spectrophotometer, USA, following the procedure described in the literature (Isaac and Hameed, 2020). Small amounts of the powdered clay samples OC, AC, and CC, respectively, were thoroughly ground with KBr, and tablets or pellets were prepared by compression under vacuum.

2.4.2 Powdered X-ray Diffractometry (PXRD)

The PXRD measurements of the clay samples were carried out in a Rigaku X-ray diffractometer (Miniflex, UK) using CuK (=0.154 nm) radiation at a scanning rate of 1 min^{-1} with an angle ranging from 10 to 80 degrees to study the composition of the clay samples.

2.4.3 Scanning Electron Microscope (SEM)

The surface morphology of the OC, AC, and CC samples was studied by a JEOL scanning electron microscope (model JSM-6390LV) at an accelerating voltage of 5–15 KV. The surfaces of the clay samples were Pt-coated before evaluation.

2.4.4 Energy Dispersive X-Ray Spectroscopy (EDS) analysis

EDS analysis was performed using an EVO 40 electron microscope (Karl Zeiss Jena, Germany) to obtain the mean elemental compositions of the samples analyzed

following the procedure described in the literature (Janek *et al*., 2009).

2.4.5 X-Ray Fluorescence (XRF) analysis

The oxide compositions of the ordinary clay (OC), acid-treated clay (AC), and calcined clay (CC) minerals were determined using the Xsupreme 8000 X-ray Fluorescence (XRF) Spectrophotometer following a literature report (Isaac *et al*., 2020; Jamo, 2016).

2.5 Data analysis

The results were expressed as mean ± SD (standard deviation). A one-way ANOVA with Tukey's HSD test was used for the analysis of the data at a significant level of $P < 0.05$. Pearson's correlation analysis was used for the analysis of the correlation among minerals and oxide compositions of OC, AC, and CC.

3.0 Results and discussion
3.1 Mineral and elemental composition of OC, AC, and CC samples

The mineral composition of the raw clay sample OC, as revealed by the PXRD result, is shown in Figs. 2(a) and (b). It is observed that the clay sample is mainly kaolin, composed of 31% quartz, *syn* (SiO_2) (a silicate mineral), 12% albite ($Na(AlSi_3O_8)$) (a plagioclase feldspar mineral of the tectosilicate class), and 1.87% orthoclase ($KAlSi_3O_8$) (an alkali feldspar mineral, a potassium aluminosilicate of the silicate class). Others include 23% muscovite ($H_2KAl_3(SiO_4)_3$) (a hydrated phyllosilicate mineral of aluminum and potassium-silicate), 11.6% nacrite ($Al_2Si_2O_5(OH)_4$) (kaolinite), 11% osumilite ($K,Na(Fe,Mg)_2(Al,Fe)_3(Si,Al)_{12}O_{30}$) (silicate mineral), and 9.7% illite ($K,H_3O)(Al,Mg,Fe)_2(Si,Al)_4O_{10}[(OH)_2,H_2O]$) (phyllosilicate mineral). Lawal *et al*. (2022) stated that kaolin is a white, soft, and plastic-hydrated aluminum silicate clay mineral composed of kaolinite, dickite, nacrite, and halloysite that is formed by the decomposition of orthoclase feldspar. The structure of kaolinite clay has been shown to consist of sheets of SiO_2 (silica) tetrahedral bonded to sheets of Al_2O_3 (alumina) octahedral (Sachan and Penumadu, 2007).

The energy dispersive X-ray spectroscopy (EDS) analyses that gave the elemental composition of the OC sample are given in Fig. 3. The chemical composition of the clay shows a high percentage of silicon (Si) (53.60%), which corresponds to quartz. The percentage of aluminum (Al) (16.40%) also indicates that it is Al-rich, which is a characteristic of muscovite. Janek *et al*. (2009) state that muscovite is an aluminum-rich variety of mica with significant K^+ alongside the Na^+ in the interlayer galleries. The percentages of other elements such as iron (Fe), calcium, and sodium (Na) were 8.50%, 3.34%, and 3.20%, respectively.

Fig. 2(a) Qualitative powdered XRD spectrum of ordinary clay sample OC

OC20230309_120618_G03_S03_M03

- Quartz, syn : 31(4)%
- Muscovite : 23(2)%
- Albite : 12(2)%
- Orthoclase : 1.87(13)%
- Osumilite : 11.0(13)%
- Illite : 9.7(16)%
- Nacrite : 11.6(19)%
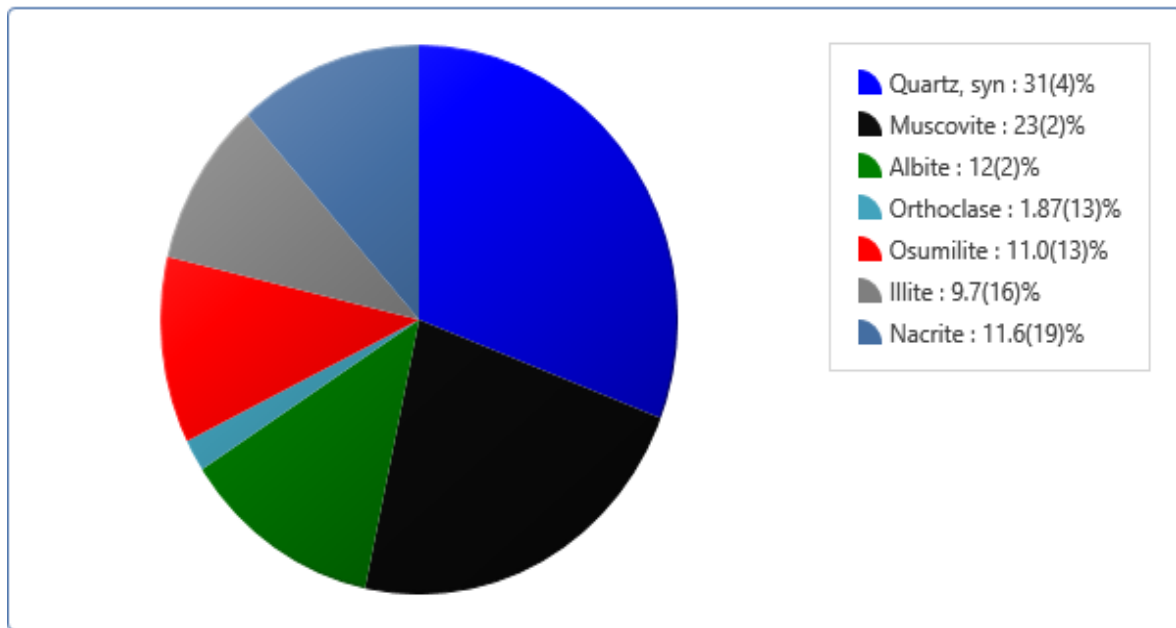
Fig. 2(b) Quantitative powdered XRD result of the ordinary clay (OC)

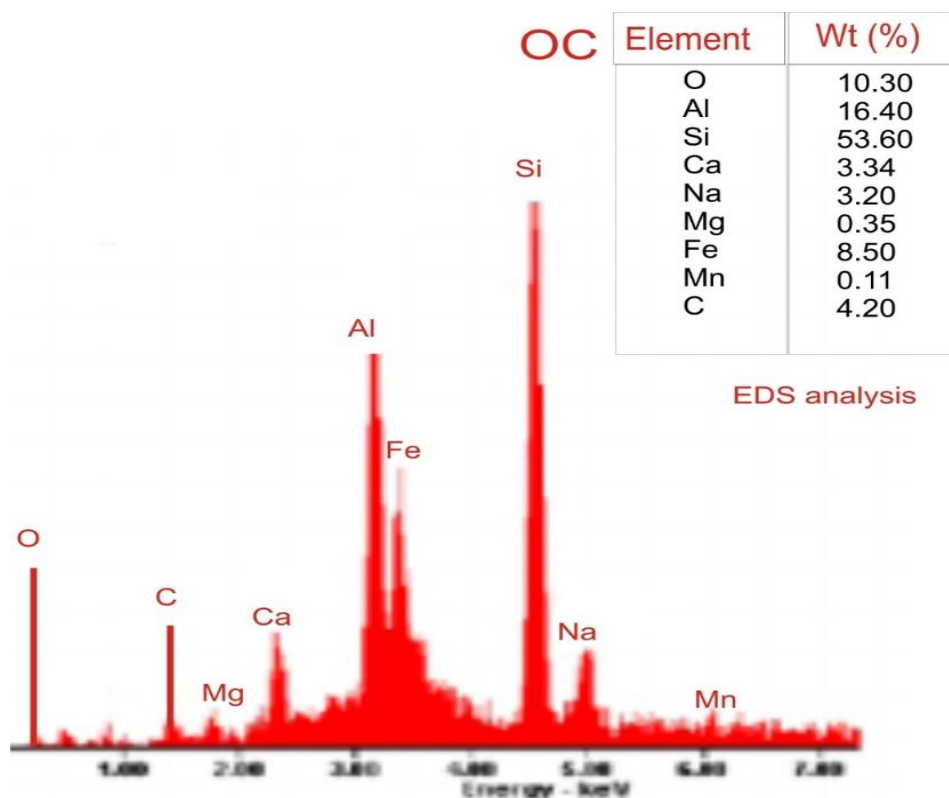| OC Element	Wt (%)
O	10.30
Al	16.40
Si	53.60
Ca	3.34
Na	3.20
Mg	0.35
Fe	8.50
Mn	0.11
C	4.20

EDS analysis

Fig. 3 EDS spectrum of OC sample

The ordinary clay sample was subjected to acid leaching using a mixture of concentrated tetraoxosulphate (VI) acid and trioxonitrate (V) acid (4:1, v/v) at ambient temperature. Under the acid-leaching condition, the XRD analysis of the clay showed that the mineral composition was slightly different. Kaolinite (8.4%) mineral formation may be from nacrite mineral that was present in the OC sample (Fig. 2b) but absent in the AC and CC samples (Figs. 4b, 6, and 7b). The percentage composition of quart (56%) and orthoclase (6%) minerals was improved by acid leaching, while those of albite (6.3%), muscovite (8.1%), illite (7%), and osumilite

(7.8%) minerals were decreased (Figs 3b and 5). Jin *et al*. (2021) stated that potassium feldspar can react with H^+ in solution, lose K^+ in the presence of H^+ and water, and form kaolinite or illite and SiO_2. This reaction also explains the sudden increase in silica content, from 68.406% in OC to 72.370% in AC, as shown in Fig. 6.

There was no significant difference at *p < 0.05* in the mineral composition between the OC and AC samples. However, the Pearson correlation coefficient shows that the minerals of sample AC were moderately positively correlated with the minerals of sample OC (R = 0.7355; R^2 = 0.541). The correlation result was significant at *p < 0.05*, and the p-value was < 0.03757. This implies that acid leaching of the clay improves the quality of the mineral composition in the clay sample.

The EDS result of the AC clay sample that shows the elemental composition of the acid-treated clay is represented in **Fig. 5**. Except Ca and Na, which were completely absent in the acid-leached clay, the other elements found in the OC sample were also present in the acid-leached clay but with varying weight percentages. This may be because the oxides of these metals reacted with the acid to convert them to soluble nitrates or sulphates. The weight percentage of Al, Si, Mg, and Fe reduces to 9.10%, 13.72%, 0.32%, and 6.52%, respectively (Fig. 5).

General information

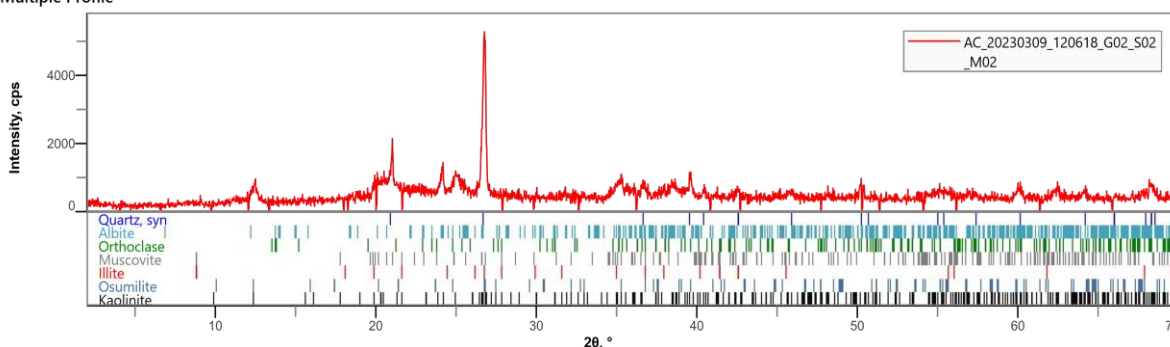| Analysis date	2023-03-09 12:47:42	Measurement start time	2023-03-09 12:11:07
Analyst	Administrator	Operator	Administrator
Sample name	AC	Comment	
Measured data name	C:\WallPaper\09-03-2023\AC_20230309_120618_G02_S02_M...	Memo	

Multiple Profile

Fig. 4(a) Qualitative powdered XRD spectrum of acid leached clay sample AC
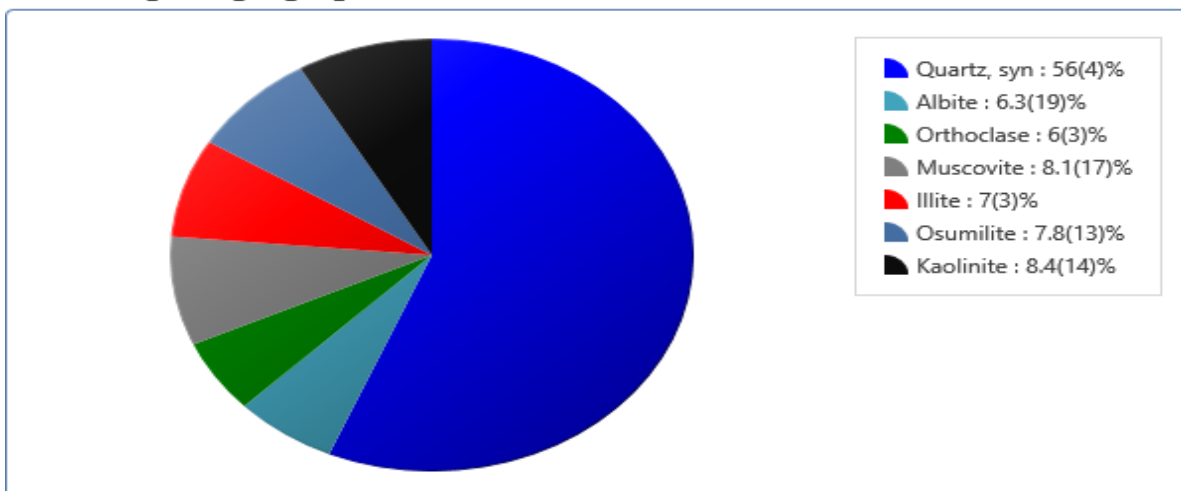

Fig. 4(b) Quantitative powdered XRD spectrum of acid leached clay sample AC
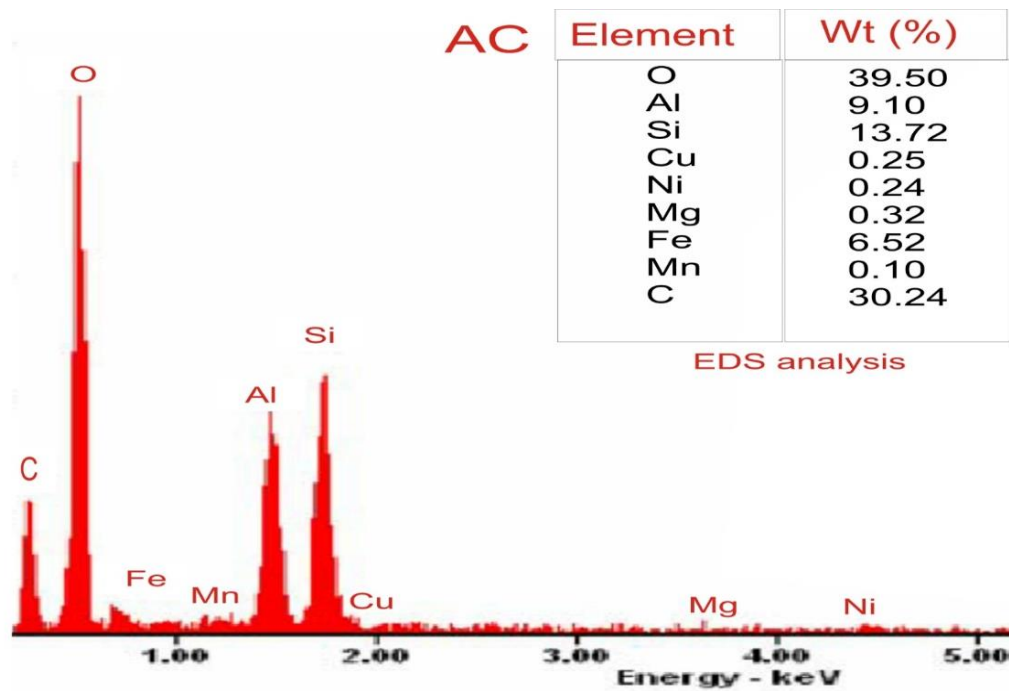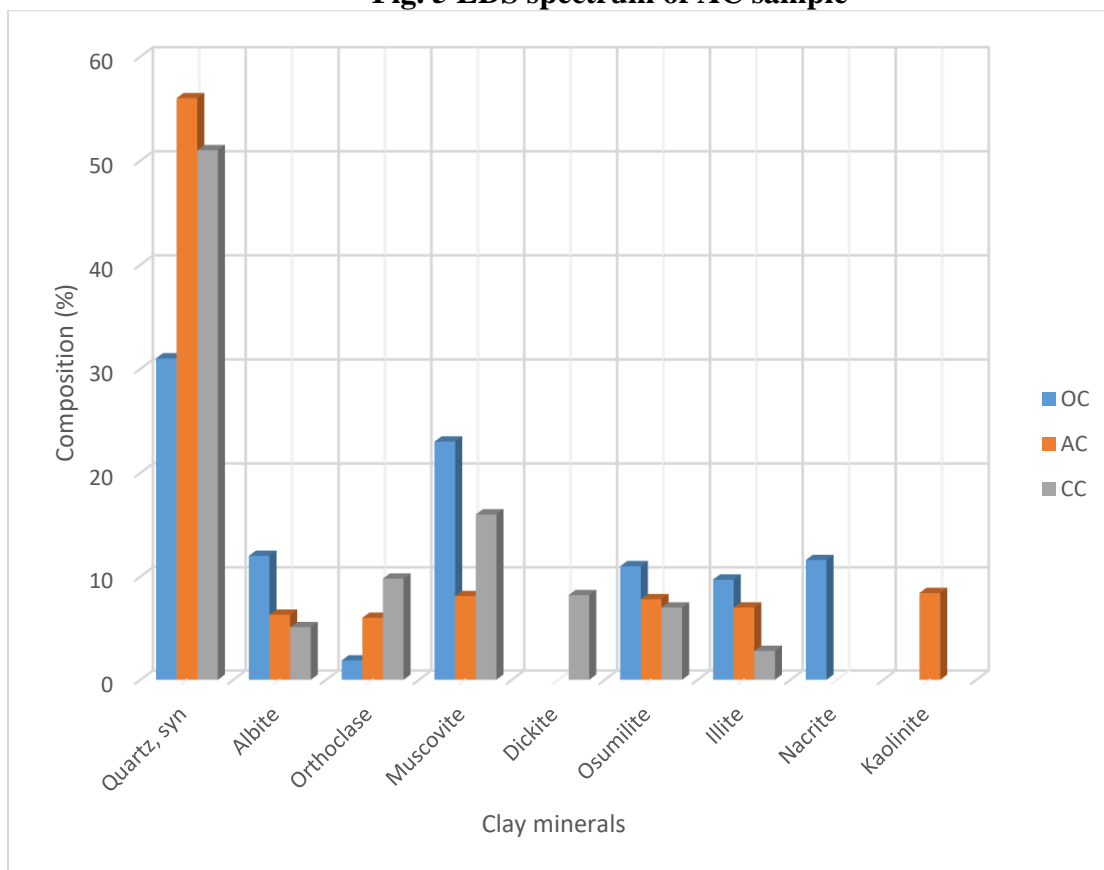
Fig. 5 EDS spectrum of AC sample

Fig. 6 Mineral composition of OC, AC, and CC clay samples

The PXRD result (Figs. 7a and 7b) of CC is unique and differs greatly from those of OC and AC. The mineral composition of CC as listed in the PXRD includes quart (51%), albite (5.1%), orthoclase (9.8%), muscovite (16%), dickite (8.2%), osumilite (7.0%), and illite (2.8%). In comparison with the mineral compositions of OC and AC, as shown in Fig. 5, the percentage of quart minerals in CC was higher than that of OC and slightly lower than

that of AC. Albite minerals were lower than those of OC and AC, while orthoclase minerals were present in high concentrations compared to those of OC and AC. Muscovite mineral content in CC was greater than that of AC and lower than that of OC. Dickite mineral was present only in the CC sample and was completely absent in the OC and AC samples. Osumilite mineral concentration decreases from OC to CC, while illite has the highest concentration of 9.7% in OC, followed by 7.0% in AC, and its concentration in CC is the lowest (2.8%) (Fig. 5). Nacrite and kaolinite minerals were completely absent in the calcined clay sample.

The elemental analysis (EDS) result (Fig. 8) shows that the weight percentage of Al of 9.10% and that of Fe of 6.52% (Fig. 13) were the same with AC. Those of Si (23.73%), Mg (1.32%), and Fe (6.52%) (Fig. 13) were higher than those obtained in the AC sample. Ca (3.25%) and Na (2.24%) that were completely absent in AC are present in CC.

There was no significant difference at $p < 0.05$ in the mineral composition among the OC, AC, and CC samples, and the p-value was 0.999958. Also, there was no significant difference at $p < 0.05$ between OC and CC mineral compositions (p-value = 0.996265) and AC and CC mineral compositions (p-value = 0.996631). However, the Pearson correlation coefficient shows that the minerals of sample CC were strongly positively correlated with the minerals of the OC sample (R = 0.774; R^2 = 0.5991). The p-value was < 0.024188, and the correlation result was significant at $p < 0.05$. There was also a strong positive correlation between AC and CC mineral compositions (R = 0.9436; R^2 = 0.8904). The p-value was < 0.00043, and the correlation results were significant at $p < 0.05$. Treatment of the clay with a mixture of strong acids eliminates the nacrite mineral and forms the kaolinite mineral. On the other hand, calcination of the clay formed another important clay mineral, dickite (Figs. 6 and 7b).

General information

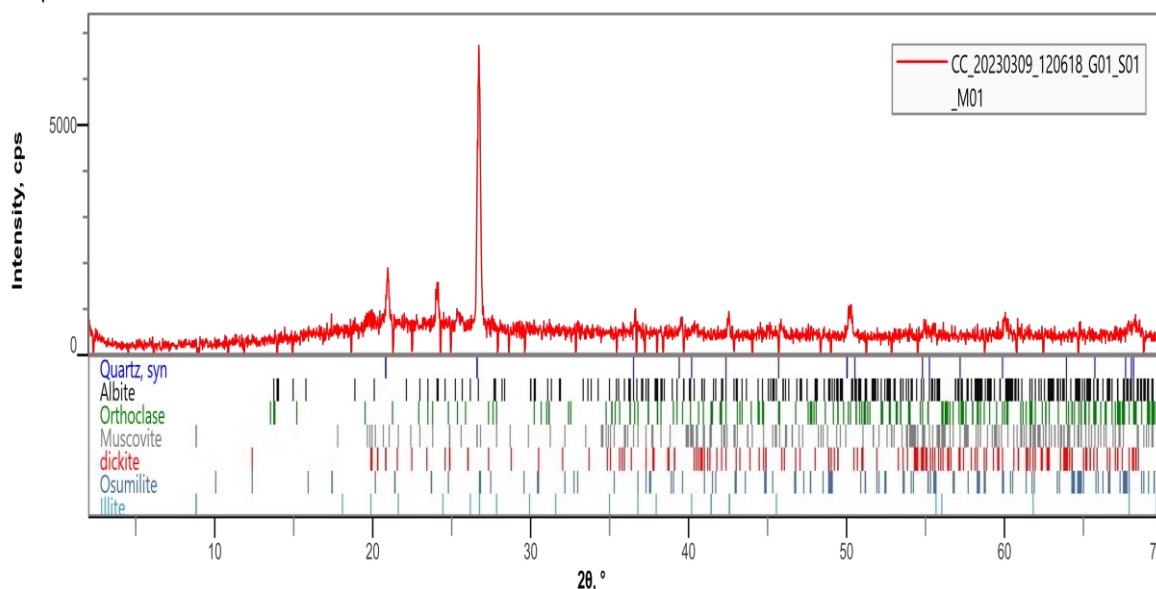| Analysis date	2023-03-09 12:53:47	Measurement start time	2023-03-09 12:07:16
Analyst	Administrator	Operator	Administrator
Sample name	CC	Comment	
Measured data name	C:\WallPaper\09-03-2023\CC_20230309_120618_G01_S01_M...	Memo	

Fig. 7(a) Qualitative powdered XRD result of calcined clay (CC)
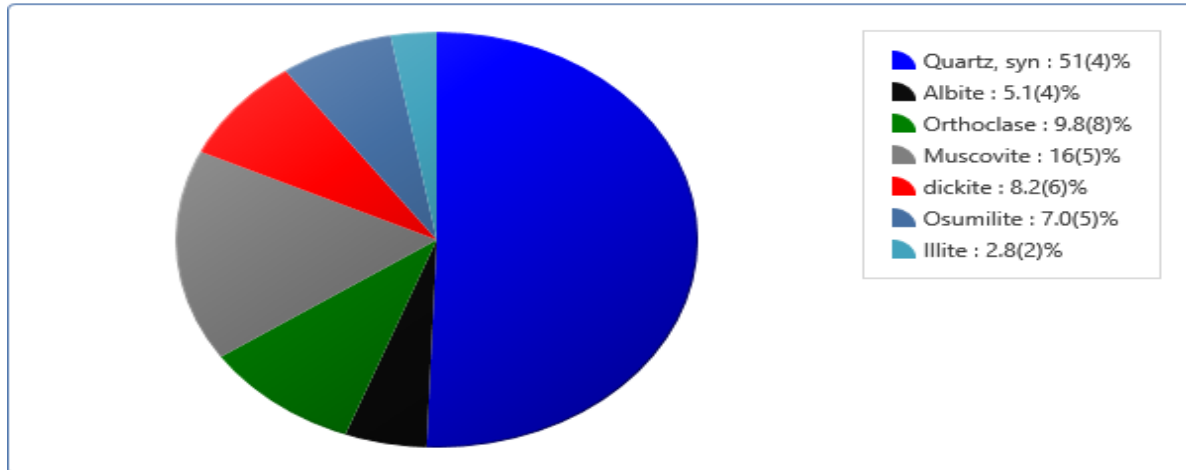
CC20230309_120618_G01_S01_M01

Quartz, syn : 51(4)%
Albite : 5.1(4)%
Orthoclase : 9.8(8)%
Muscovite : 16(5)%
dickite : 8.2(6)%
Osumilite : 7.0(5)%
Illite : 2.8(2)%

Fig. 7(b) Quantitative powdered XRD result of calcined clay (CC)

CC

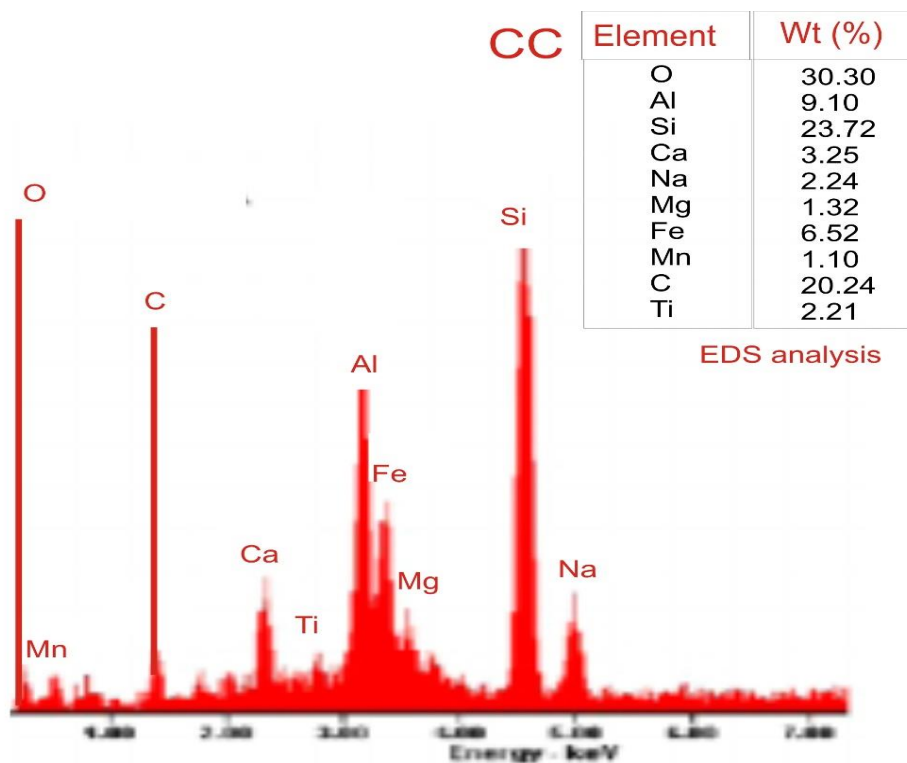| Element	Wt (%)
O	30.30
Al	9.10
Si	23.72
Ca	3.25
Na	2.24
Mg	1.32
Fe	6.52
Mn	1.10
C	20.24
Ti	2.21

EDS analysis

Fig. 8 EDS spectrum of CC sample

3.2 Oxides composition of OC, AC, and CC samples

The major oxides present in the OC clay mineral as obtained by XRF analysis (Fig. 9) include quart with the highest percentage of 68.406%, followed by Al_2O_3 (20.175%), Fe_2O_3 (3.254%), TiO_2 (2.885%), CaO (1.506%), K_2O (1.226%), and SO_3 (0.449%). The percentage composition of other oxides such as V_2O_5, Cr_2O_3, MnO, NiO, CuO, ZnO,

Ag2O, and Ce_2O (Fig. 9) was insignificant among OC, AC, and CC samples.

There was no significant difference at $p < 0.05$ in the oxide composition between the OC and AC samples. But the Pearson correlation coefficient shows that the oxides of sample AC were strongly positively correlated with the oxides of sample OC (R = 0.9992; R^2 = 0.9984). The correlation result was significant at $p < 0.05$, and the p-value is < 0.00001. This implies that acid leaching of

the clay improves the quality of the oxide composition in the clay sample.

With the exception of SiO_2, which has the highest percentage composition of 73.663% when compared with those of OC and AC samples (Fig. 9), the oxide composition of the CC sample was similar to that of OC and AC, but its percentage composition was smaller compared to that obtained for OC and AC.

Acid treatment of the clay sample has improved the percentage composition of some oxides, such as SiO_2 of 72.370%, K_2O of 1.432%, and TiO_2 of 3.145%. While the composition of other oxides such as Fe_2O_3 (1.513%), CaO (0.341%), and Al_2O_3 (19.414%) decreases (Fig. 9). This may be attributed to the possibility of these oxides reacting with the acid during acid leaching.

There was no significant difference at $p < 0.05$ in the oxide composition among the OC, AC, and CC samples, and the p-value was 1. There was also no significant difference at $p < 0.05$ between OC and AC oxides (p-value = 0.999688), OC and CC oxides (p-value = 1), and AC and CC oxides (p-value = 0.999698). But the Pearson correlation coefficient shows that the oxides of sample CC were strongly positively correlated with the oxides of OC sample (R = 0.9987; R^2 = 0.9974) and AC sample (R = 9992; R^2 = 0.9984), and AC and CC oxides (R = 0.9998; R^2 = 0.9996). The p-values were < 0.00001, and the correlation results were significant at $p < 0.05$. This also verifies that treatment of the clay sample via acid leaching and calcination improves the quality of the oxides in the clay mineral.
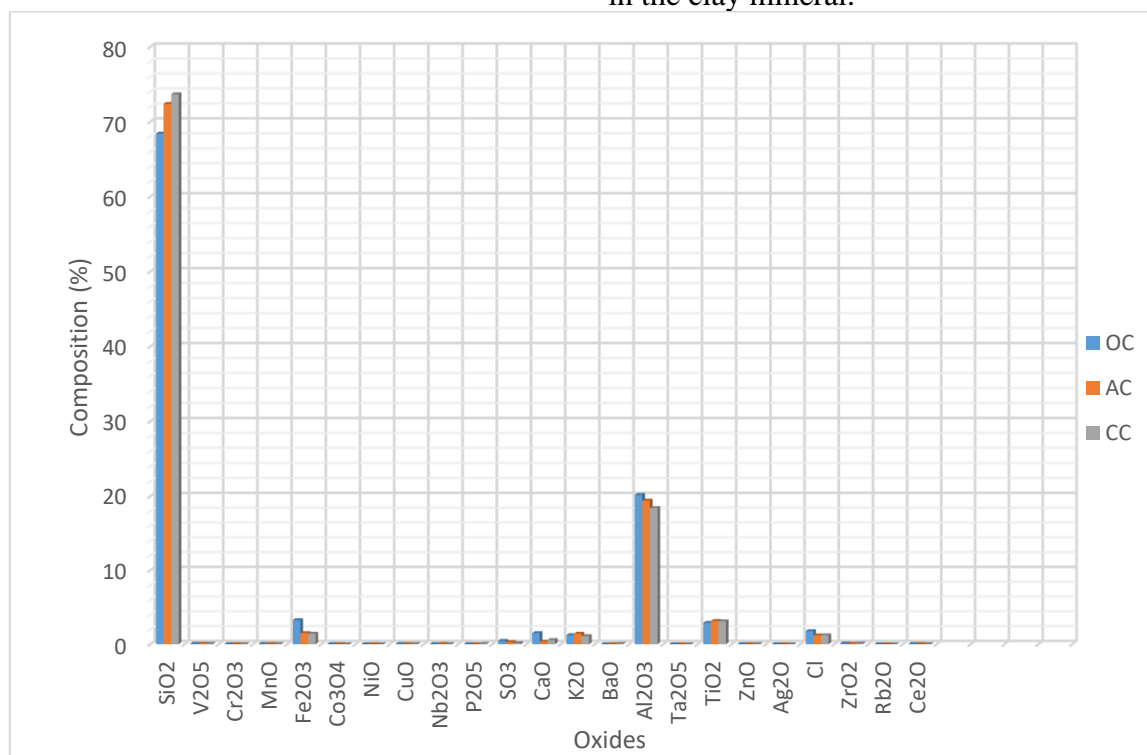
Fig. 9 Oxides composition of ordinary clay (OC), acid-leached clay (AC) and calcined clay (CC)

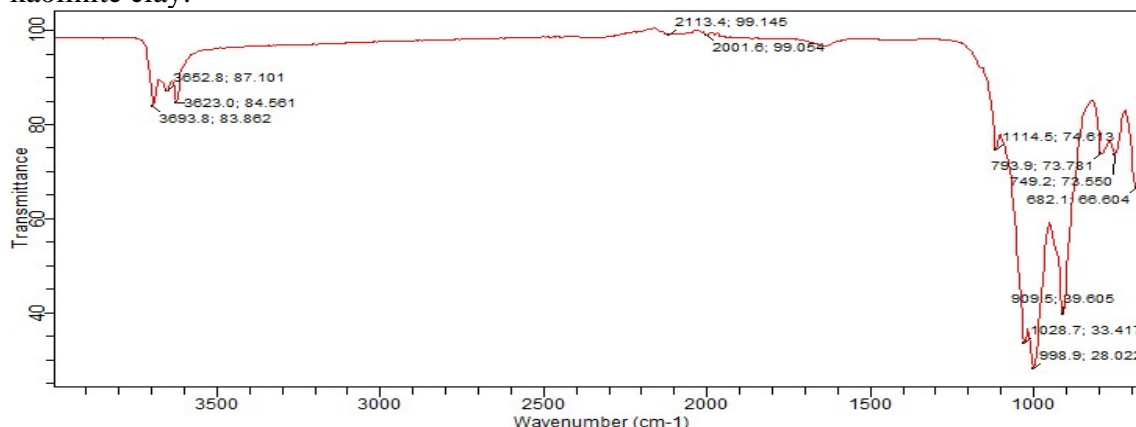### 3.3 Functional group analysis of OC, AC, and CC samples

Fig. 10 shows the FT-IR absorption spectra of the ordinary clay (OC) sample obtained at Ikot Ekang, Etinan L. G. A., Nigeria. The absorption bands at 682.1, 749.2, and 793.9 cm^{-1} with correlation intensities of 66.604,

73.550, and 73.781, respectively, indicate that the sample is quartz-rich. The absorption at 793.9 cm^{-1} also indicates the presence of carbonates, Si-O stretching, Si-O-Al stretching, (Al, Mg)-OH, and Si-O-(Mg, Al) in the clay sample. Al-O-Al stretching is indicated at the absorption band of 749.2 cm^{-1}. The absorption band at 682.1 cm^{-1} represents Si-O deformation. The absorption

band at 998.9 cm^{-1} with an intensity of 28.022 indicates Si-O stretching equally. Janek *et al.* (2009) reported an absorption band of 698 cm^{-1} for Si-O deformation in phlogopite, 681 cm^{-1} for Mg$_3$-OH deformation in biotite, and 3654 cm^{-1} for Mg$_2$Al-OH stretching. The absorption band at 1114.5 cm^{-1} indicates the presence of sulphates in the clay sample. The sulphates are demonstrated to have strong absorption bands near 980 cm^{-1}, 450 cm^{-1}, 1150–1100 cm^{-1}, and 675–590 cm^{-1} (Jozanikohan and Abarghooei, 2022).

The absorption band at 3623.0 cm^{-1} with a correlation intensity of 84.561 indicates the stretching vibration of the surface hydroxyl group of kaolinite (1:1 layer) clay, while the absorption band at 3652.8 cm^{-1} with a correlation intensity of 87.101 represents illite (2:1 layer) and smecite of kaolinite clay. The absorption band at 3693.8 cm^{-1} with a correlation intensity of 83.862 corresponds to the vibration of the inner OH group of kaolinite clay.

The presence of these absorption bands for OH at 3623–3693.8 cm^{-1} is a characteristic of kaolinite clay. This implies that the OC sample is mainly kaolin clay. Djomogoue and Nyopwouo (2013) reported that the stretching vibrations of surface OH groups are assigned the band at 3652, 3671, and 3694 cm^{-1}, while the vibrations at 3620 cm^{-1} are attributed to the inner OH groups. The main distinctions of kaolinite-group minerals are observed in the presence of two narrow and intensive OH stretching absorption peaks around 3650 and 3666 cm^{-1}, which are characteristic of an ordered variety of kaolinite (Khang *et al.*, 2016). Predictions of the differences in the chemical composition based on FTIR spectroscopy in Fig. 10 were also confirmed by the energy dispersive X-ray spectroscopy (EDS) analyses that show the percentages of the different elements present in sample OC (Fig. 3).

Fig. 10. FTIR result of ordinary clay (OC) sample

The FT-IR of the acid-treated clay (AC) is shown in **Fig. 11**. There is much similarity between this FT-IR and the FT-IR of the OC clay sample. The absorption bands and their corresponding correlation intensities at 3623.0 cm^{-1} (85.891) indicating the stretching vibration of the surface hydroxyl group of kaolinite (1:1 layer) clay, 3652.8 cm^{-1} (88.295) representing illite (2:1 layer) and smecite of kaolinite clay, and 3693.8 cm^{-1} with an intensity of 84.608 corresponding to the vibration of the inner OH group of

kaolinite clay were also noticed in FT-IR of OC. The slight difference is seen in the correlation intensities of the absorption bands, which in AC are slightly higher than those in OC. There is also an absorption band at 1028.7 cm^{-1} with a correlation intensity of 27.529, representing Si-O-Si and Si-O stretching, and at 1636.3 cm^{-1} with a correlation intensity of 96.524, indicating H-O-H stretching. Other absorption bands were similar to those obtained in the IR of the OC clay sample.

The FT-IR results of AC show that treatment of the clay mineral with mineral acid does not

change the actual composition of the clay but has improved its performance properties.
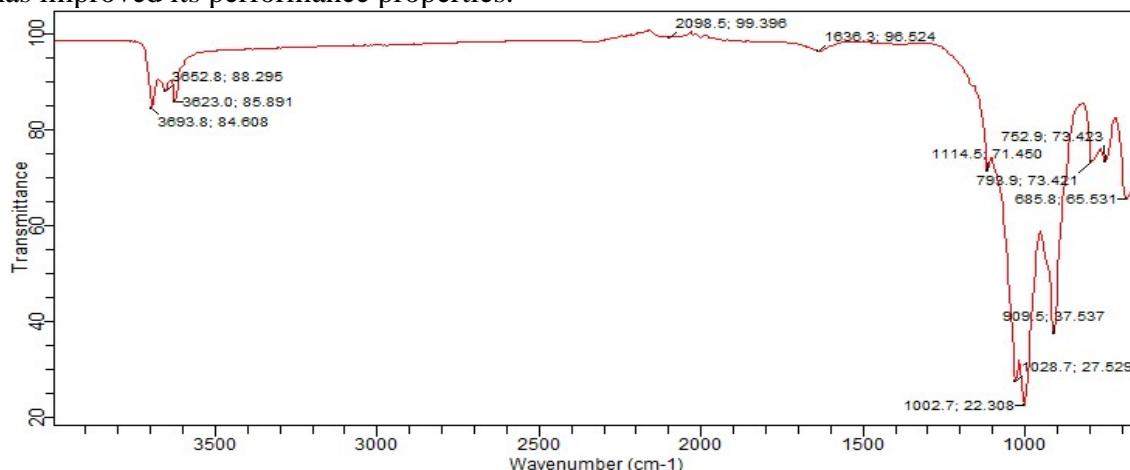
Fig. 11 FT-IR of acid activated clay (AC) sample

The acid-activated clay was subjected to calcination by heating it in a furnace at 1050 °C for 2 hours. The FTIR of the calcined clay (CC) sample is shown in Fig. 12. The IR spectrum of CC is completely different from those of OC and AC. The absorption bands within the region of 3623–3695 cm^{-1}, representing the hydroxyl groups of kaolinite-group minerals, were completely absent. The absorption bands at 693.3 cm^{-1} with a correlation intensity of 73.709 and 775.3 cm^{-1} with a correlation intensity of 72.376 represented Si-O stretching and Si-O-Al stretching, respectively. The absorption band at 1047.4 cm^{-1} (60.791) represented Si-O-Si and Si-O stretching. H-O-H stretching, or OH deformation of water, was found at 1636.3 cm^{-1} with 98.704 as correlation intensity. Generally, the FTIR result of the CC sample showed that calcination, to a greater extent, has been able to remove the water molecules that could be found within the clay layers and basically form silica. This observation corroborates the literature report (Ekpa and Isaac, 2008).
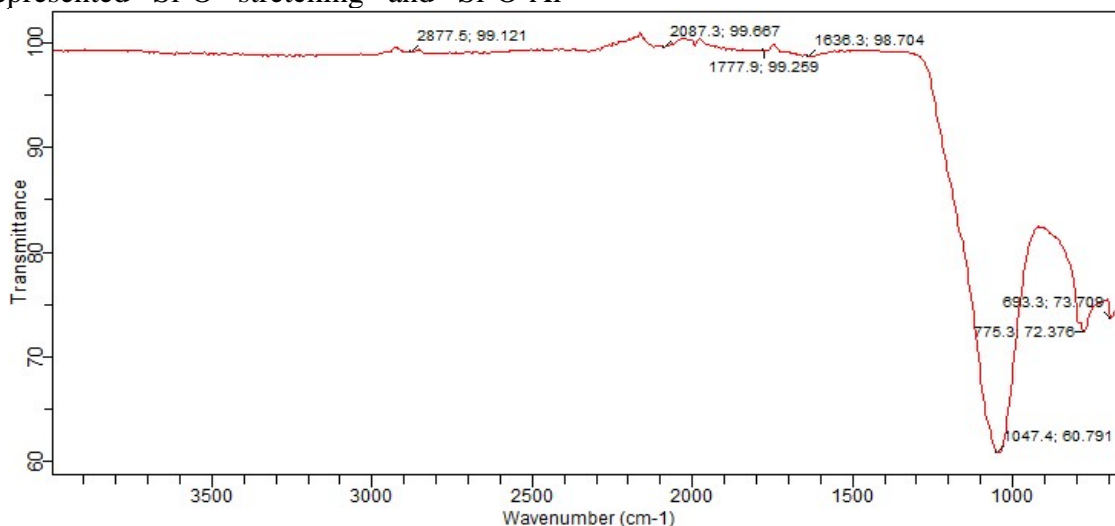
Fig. 12 FTIR result of the calcined clay (CC)

### 3.4 Surface morphology of OC, AC, and CC samples

The surface morphology of the ordinary clay sample OC at different magnifications is shown in Fig. 13. The SEM images had a plate-like shape with a pseudo-hexagonal structure of 5–10 μm in size and aggregate layers of non-uniform-size euhedral particles. This shows a very large size-to-thickness

ratio. Sachan and Penumadu (2007) made a similar observation of clay platelets on the top surface aligning themselves with their faces along the surface with the particles existing under the topmost surface in random microfabric (face-to-edge particle contact).
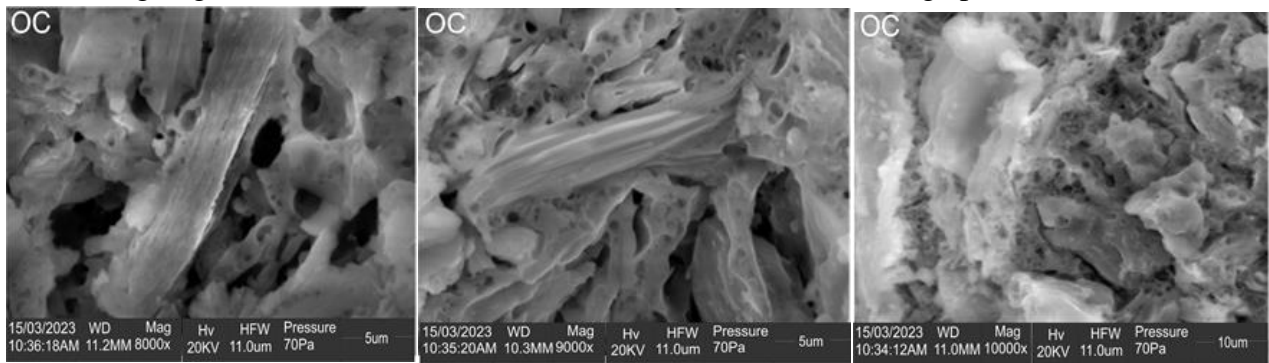
Fig. 13 SEM results of ordinary clay (OC) sample

SEM images of the AC sample are shown in Fig. 14. It is clear from Figure 14 that the leaching of the clay with the mixture of acids has increased the porosity of the clay sample, with the kaolinite mineral playing a vital role as pore-filling clay minerals and illite as microfibers. The SEM result also shows platymorphology. Kaolinite clay was identified as a pore-filling clay mineral and illite as microfibers during the Fourier transform infrared spectroscopy (FTIR) analysis for the clay mineralogy studies in a clastic reservoir (Jozanikohan and Abarghooei, 2022).
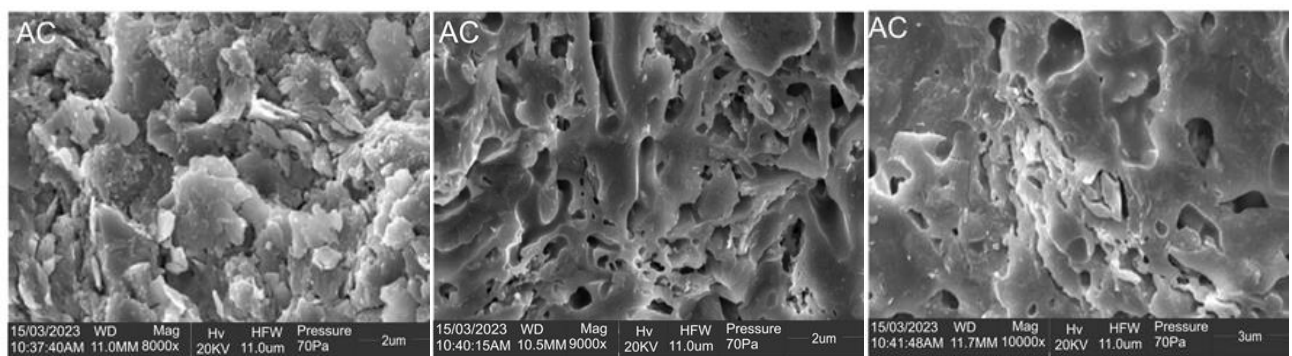
Fig. 14 SEM results of acid leached clay (AC) sample

The surface morphology of CC shown in Fig. 15 seems to be smother, highly porous, and not platy as in the OC and AC surfaces. This implies that calcination has reduced the clay's particle size to a greater extent and increased the porosity of the clay material.
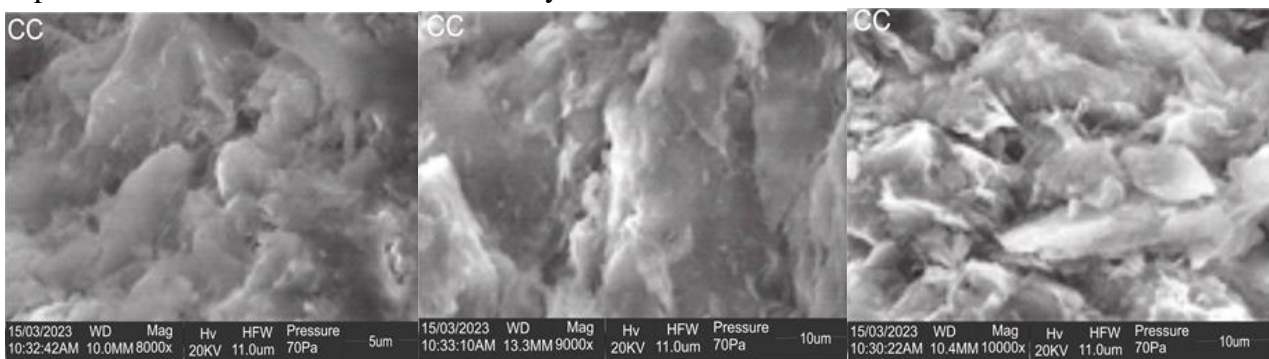
Fig. 15 SEM results of calcined clay (CC) sample

4.0 Conclusion

Clay minerals from southern Nigeria are mainly kaolinite clay, consisting of minerals such as quart, *syn*, albite, orthoclase, muscovite, nacrite, osumilite, and mulite. The SEM images for the surface morphology show that it has a plate-like shape with a large size-to-thickness ratio. The major oxides present were SiO_2, Al_2O_3, Fe_2O_3, TiO_2, CaO, K_2O, and SO_3.

The acid leaching of the clay converted nacrite minerals into kaolinite minerals. Treatment of the clay with the mixture of conc. H_2SO_4 and HNO_3 increases the percentage composition of SiO_2, K_2O, and TiO_2 oxides and decreases those of Fe_2O_3, CaO, and Al_2O_3.

Calcination of the clay at 1050 °C completely removed the OH groups of the kaolinite-group minerals. The calcined clay was mostly silica. The minerals present were quart, albite, orthoclase, muscovite, dickite, osumilite, and illite.

5.0   References

Cai, X.L., Li, C.J., Tang, Q., Zhen, B.W., Xie, X.L., Zhu, W.F., Zhou, C.H., & Wang, L.J. (2019). Assembling kaolinite nanotube at water/oil interface for enhancing pickering emulsion stability. *Appl. Clay Science*, 172, pp. 115–122.

Chougan, M., Ghaffar, S. H., Nematollahi, B., Sikora, P., Dorn, T., Stephen, D., Alber, A., & Al-Kheetan, M. J. (2022). Effect of natural and calcined halloysite clay minerals as low-cost additives on the performance of 3D-printed alkali-activated materials. *Materials & Design.*, 223, pp. 11188. https://doi.org/10.1016/j.matdes.2022.11 1183.

Djomgoue, P., & Njopwouo, D. (2013). FT-IR spectroscopy applied for surface clays characterization. *Jour. Surface Engineered Mate. & Adv. Technology*, 3, pp. 275-282.

Ekpa, O.D., & Isaac, I.O. (2008). The effect of mineral acids (HCl, H_3PO_4) on the bleaching property of clay on palm oil. *New Era Res. Jour. Eng. Sci. & Tech.*, 1, 2, pp.141-150.

Ewis, D., Ba-Abbad, M. M., Benamor, A., & El-Naas, M. H. (2022). Adsorption of organic water pollutants by clays and clay minerals composites: A comprehensive review. *Appl. Clay Science*, 229, pp. 106686. https://doi.org/10.1016/j.clay.2022.1066 86

Gao, P., He, Z.I., Gary, G.L., Li, S.J., Xiao, X.M., Han, Y.Q., & Zhang, R.Q. (2020). Mixed seawater and hydrothermal sources of nodular chert in Middle Permian limestone on the eastern Paleo-Tethys margin (South China). *Palaeogeogr. Palaeoclimatol. Palaeoecology*, 55, pp. 1–17.

Gogoi, P., Boruah, M., Bora, C., & Dolui, S. K. (2014). *Jatropha curcas* oil based alkyd/epoxy resin/expanded graphite (EG) reinforced bio-composite: Evaluation of the thermal, mechanical and flame retardancy properties. *Prog. Org. Coating*, 77, pp. 87-93.

Isaac, I. O., & Hameed, A. (2020). Synthesis of pharmacologically active hexahydroacridine-1, 8 (*2H*, *5H*)-diones using nickel (II) fluoride tetrahydrate as a new heterogeneous catalyst. *Communication in Physical Science*, 5, 2, pp. 83-98.

Isaac, I. O., Uwanta, E. J., Obadimu, C. O., & Etuk, G. E. (2020). Performance analysis of inactivated and acid activated marine and terrestrial shells based adsorbent as an alternative bleaching material for palm oil. *Sensor Letters*, 18, pp. 1-10.

Isaac, I. O., Willie, I. E., & Thompson, Q. S. (2022b). Studies on the utilization of *Hura crepitans* seed oil, aqueous extract of *Curcuma longa* L., aluminum, and magnesium metallic soaps in the preparation of emollient cream. *Researchers Jour. Sc. & Technology*, 2, 3, pp. 18-27.

Isaac, I.O., Etesin, U.M., Nya, E.J., Ukpong, E.J., Isotuk, U.G., & Ibok, U.J. (2022a). Ethnobotanical study, phytochemical composition and in vitro antioxidant activity of the methanol extracts of thirty-two medicinal plants from Southern

Nigeria. *Jour. Med. Plants Research*, 16, 10, pp. 288-299.

Jamo, H. U. (2016). Structural analysis and surface morphology of quartz. *Bayero Jour. Pure & Appl. Science*, 9, 2, pp. 23 0 – 233.

Janek, M. N., Buga, I., Lorenc, D., Szocs, V., Velic, D., & Chorvat, D. (2009). Terahertz time-domain spectroscopy of selected layered silicates. *Clays & Clay Minerals*, 57, 4, pp. 416–424.

Jin, X., Chen, L., Chen, H., Zhang, L., Wang, W., Ji, H., Deng, S., & Jiang, L. (2021). XRD and TEM analyses of a simulated leached rare earth ore deposit: Implications for clay mineral contents and structural evolution. *Ecotoxicol. & Environ. Safety*, 225, pp. 112728. https://doi.org/10.1016/j.ecoenv.2021.11 2728.

Jozanikohan, G., & Abarghooei, M. N. (2022). The Fourier transform infrared spectroscopy (FTIR) analysis for the clay mineralogy studies in a clastic reservoir. *Jour. Petrol. Exploration & Prod. Technology*, 12, pp. 2093–2106.

Khang, V. C., Korovkin, M. V., & Ananyeva, L. G. (2016). Identification of clay minerals in reservoir rocks by FTIR spectroscopy. *IOP Conf. Series: Earth & Environ. Science*, 43, pp. 012004. DOI:10.1088/1755-1315/43/1/012004

Lawal, J. A., Odeyemi, O. T., Anaun, T. E., & Omotehinwa, F. H. (2022). Characterization and potential industrial applications of kaolinite from Argungu, Kebbi State, Nigeria. *Int. Jour. Scientific & Eng. Research*, 13, 4, pp. 776 – 791.

Lei, H., Huang, W., Jiang, Q., & Luo, P. (2022). Genesis of clay minerals and its insight for the formation of limestone marl alterations in Middle Permian of the Sichuan Basin. *Journal Petroleum Science & Engineering*, 218, pp. 111014. https://doi.org/10.1016/j.petrol.2022.111 014

Li, J., Cai, Z., Chen, H., Cong, F., Wang, L., Wei, Q., & Luo, Y.J.P. (2018). Influence of differential diagenesis on primary depositional signals in limestone-marl alternations: An example from Middle Permian marine successions, South China. *Palaeogeogr. Palaeoclimatol. Palaeoecology*, 495, pp. 139–151.

Nascimento, G. M. D. (2016). Structure of clays and polymer–clay composites studied by X-ray absorption spectroscopies. In: Clay, Clay Minerals and Ceramic Materials Based on Clay Minerals (eds. G.M.D. Nascimento), ExLi4EvA, ISBN-10:953-51-2259-2.

Panda, B., Unluer, C., & Tana, M. J. (2019). Extrusion and rheology characterization of geopolymer nanocomposites used in 3D printing. *Composites Part B*., 176, pp. 107290. https://doi.org/10.1016/j.compositesb.20 19.107290.

Pour-Esmaeil, S., Qazvini, N. T., & Mahdayi, H. (2014). Interpenetrating polymer networks (IPN) based on gelatin/poly(ethylene glycol) dimethacrylate/clay nanocomposites: Structure-properties relationship. *Mat. Chm & Physics*, 143, pp. 1396-1403.

Ruiz, A. I., Ruiz-García, C., & Ruiz-Hitzky, E. (2023). From old to new inorganic materials for advanced applications: The paradigmatic example of the sepiolite clay mineral. *Appl. Clay Science*, 235, pp. 106874. https://doi.org/10.1016/j.clay.2023.1068 74

Sachan, A., & Penumadu, D. (2007). Identification of microfabric of kaolinite clay mineral using X-ray diffraction technique. *Geotech. Geol. Engineering*, 25, pp. 603–616.

Shi, K., Chen, J., Pang, X., & Jiang, F. (2023). Wettability of different clay mineral surfaces in shale: Implications from molecular dynamics simulations. *Petroleum Science*, https://doi.org/10.1016/j.petsci.2023.02.0 01.

Stocchi, E. (1990). Industrial Chemistry (Vol.1). Ellis Horwood Ltd, England.

Su, C.P. Li, F., Tan, X.C., Gong, Q.L., Zeng, K., Tang, H., Li, M.L., & Wang, X.F.

(2020). Recognition of diagenetic contribution to the formation of limestone-marl alternations: A case study from Permian of South China. *Mar. Petrol. Geology*, 111, pp 765–785.

Wang, S., Gainey, L., Mackinnon, I.D.R., Allen, C., Gu, Y., & Xi, Y. (2022). Thermal behaviors of clay minerals as key components and additives for fired brick properties: A review", *Jour. Building Engineering*, 66, pp 105802. doi.org/10.1016/j.jobe.2022.105802.

Worrall, W.E. (1982). *Ceramic raw materials* (2nd revised ed.), Pergamon Press, UK.

Wu, Z., Chen, Y., Wang, Y., Xu, Lin, Y., Liang, Z. X., & Cheng, H. (2023). Review of rare earth element (REE) adsorption on and desorption from clay minerals: Application to formation and mining of ion-adsorption REE deposits. *Ore Geo. Reviews*, 157, pp. 105446. https://doi.org/10.1016/j.oregeorev.2023.105446.

Xu, F., Onel, O., Council-Troche, M., Noble, A., Yoon, R.H., & Morrisa, J.R. (2021). A study of rare earth ion-adsorption clays: The speciation of rare earth elements on kaolinite at basic pH. *Appl. Clay Science*, 201, pp. 105920. doi.org/10.1016/j.clay.2020.105920

Compliance with Ethical Standards

Declarations
The authors declare that they have no conflict of interest.

Data availability
All data used in this study will be readily available to the public.

Consent for publication
Not Applicable.

Availability of data and materials
The publisher has the right to make the data public.

Competing interests
The authors declared no conflict of interest.

Author's contribution
Ukeme O. Isaac: Methodology, software, writing-reviewing and editing
Ibanga O. Isaac: Conceptualization, writing-original draft preparation
Itoro E. Willie: Data curation, software, formal analysis
Etiyene I. Essiet: Investigation, validation, resources
Rasheed Babalola: Visualization, project administration
Udo J. Ibok: Supervision, writing-reviewing and editing